Grant No. DE-FG02-03ER83720 between MULTIMAX, Inc. and U.S. Department of Energy

SUMMARY

Effective and reliable nuclear monitoring requires discrimination between small magnitude explosions and earthquakes based on the use of limited regional data. Lg is generally the largest seismic phase from both explosion and earthquake sources recorded at regional distances. For small events, Lg may sometimes be the only well-recorded seismic phase so that discriminants based only on the use of Lg are especially desirable. Recent research has provided significantly better understanding of Lg by demonstrating that the explosion-generated Rg makes significant contribution to the low-frequency S or Lg from explosions. Near-source scattering of explosion-generated Rg appears to be a viable mechanism for generating low-frequency (< 2 Hz) Lg waves from explosions. Detailed knowledge of the complex scattering process is, however, still incomplete and is in fact the subject of several ongoing studies.

Our analysis of regional data from nuclear explosions from both Nevada Test Site (NTS) and Kazakh Test Site (KTS) and nearby earthquakes in Phase I has suggested that there are several reliable source discrimination methods only based on the use of Lg at regional distances. These discriminants should be especially useful for small magnitude seismic events for which Lg may be the only well-recorded seismic phase. Our results suggest four possible regional discriminants: (a) frequency-amplitude-time analysis of spectrograms, (b) Lg(low frequency)/Lg(high frequency), (c) Lg spectral slopes, and (d) skewness of Lg spectra. Remarkable similarity of discrimination results from both NTS and KTS nuclear explosions and nearby earthquakes, with entirely different geological settings, indicates that our results should be applicable to other regions of the world.

1. INTRODUCTION

Lg is generally the largest seismic phase from both explosion and earthquake sources recorded at regional distances. For small events, Lg may sometimes be the only well-recorded seismic phase. It is therefore important to develop a reliable source discrimination method based on the use of only the Lg phase. Gupta et al. (1992) provided observations and theoretical model suggesting that near-source scattering of explosion-generated Rg into S makes a significant contribution to the low-frequency (less than 2 Hz) Lg. This mechanism explains why the low-frequency Lg from explosions is so large that it destroys the discrimination capability of Pn/Lg amplitude ratios at a frequency of ~1 Hz. Observational support for this mechanism has grown in recent years (Patton and Taylor, 1995; Gupta et al., 1997; Myers et al., 1999, Patton, 2000, 2001). A study of broadband regional waveforms from Nevada Test Site (NTS) explosions and earthquakes by Woods and Helmberger (1997) also led them to conclude that the S-wave generation is mainly caused by near-source scattering, which is highly dependent on the near-source geology.

Several more recent studies, such as Bonner et al. (2003), Myers et al. (2003), and Wu et al. (2003), also provide strong evidence in favor of the Rg-to-S scattering mechanism for the generation of the low frequency S and Lg. According to Myers et al. (2003), "Despite pervasive use of S-phases in seismic monitoring, generation of regional S-waves from explosive (P- wave) sources is not well understood. Most investigators agree that appreciable energy from explosion sources is converted to S-waves near the source, but the dominant P-to-S transfer mechanism is not agreed upon. With the exception of surface-wave scattering, supporters of each mechanism describe them analytically, and each mechanism can be used to fit a subset of observations. However, surface-wave scattering, the only mechanism without an adequate analytical

representation, offers an explanation for some of the most intriguing regional S-wave observations."

2. COLLECTION OF DATA

We selected a large number of regional waveform data for nuclear explosions and earthquakes recorded at the four stations, Mina (MNV), Kanab (KNB), Landers (LAC), and Elko (ELK) of the Lawrence Livermore National Laboratory's (LLNL) network from our pre-existing stock of waveform data. Most of the nuclear events came from the Yucca Flats region of the Nevada Test Site (NTS), which included a wide range of shot depths and yield values, and included several closely spaced explosions.

We also restored 22 MB of waveform data in SAC format for 38 nuclear explosions in Lop Nor, China and E. Kazakhstan from 1987-1996 and 32 earthquakes from 1992-1995 at stations AAK and WMQ, a dataset that was sent to us by Steve Taylor. These data from several geologically distinct regions are helpful in understanding the discrimination characteristics of the Lg wavetrain and other regional phases under varying near-source environments.

3. Spectrogram Software Development

A revised version of the spectrogram tool in MatSeis, the MATLAB-based seismic analysis software package created by Sandia National Lab, has been developed. A comparison with results based on the use of SAC2000 indicated a timing error in the latter. An option for a noise correction to be applied to the signal power spectral density, in which the noise window can be specified as a multiple of the moving FFT signal window, has been added. Any negative data values, obtained by subtracting the noise, are all set to zero.

The spectool input GUI window in MatSeis has been expanded to provide a variety of options, including plotting routines. For example, a new filled contour plot option is available in addition to the original image pixel plot. The former can now be plotted with or without contour lines. The lower and upper frequency limits can be specified and three types of spectra can be plotted, including power, amplitude, or magnitude in log (DB) units. Waveforms can be plotted above the spectrogram with corresponding time scales. The time scales can be displayed with absolute time (HH:MM:SS) or reduced time relative to origin time or waveform start time. As an alternative to the "low frequency" (1/window length) and percent overlap inputs, the user can instead provide the window and slice parameters in seconds. Other features include a smoothing option for the spectrogram and input parameters to cut the time window displayed (although the spectrogram is calculated using the entire waveform). Lastly, a title can be entered.

New features in spectool now include a sonogram option. Similar to the procedure in SAC2000, a sonogram is calculated as the difference between two smoothed versions of the same spectrogram. The narrow and wide frequency bandwidths (Hz) spectrograms are computed, and the wide band spectrogram values, representing background, are subtracted from those from the narrow band. Several different weighting schemes were tried. The most satisfactory weighting procedure appeared to be the following: (a) Narrow band spectrogram: each frequency is centered symmetrically within an odd number of data points; the central frequency is given the highest weight of one and the adjacent frequencies on each side are assigned less and less weight as they go farther from the central frequency. (b) Wide band spectrogram: same as the narrow band except that the central frequency is zero-valued in order to enhance local sharp peaks, when the wide band values are subtracted from the narrow band values. As a result, not only the zero

and Nyquist frequency data points, but also the points adjacent to these two frequencies are dropped.

These improved and corrected versions of MATSEIS-based spectrograms and sonograms, with optional noise correction, have been found to be very useful for this SBIR project.

4. Discrimination Based on Analysis of Spectrograms

Spectrograms of underground nuclear explosions recorded at regional distances generally show the Lg wavetrain to consist of several distinct low-frequency arrivals with progressively lower frequency content and diminishing strength or amplitude. The most probable reasons for this are: the scattering of explosion-generated Rg into S occurs at several discrete near-source locations at different distances from the source, Rg has a significantly lower propagation velocity as compared to that of Lg, and Rg suffers considerably larger attenuation with distance than Lg. On the other hand, Lg wavetrains on earthquake sonograms do not show such characteristics.

A spectrogram may be considered as a three-dimensional matrix of numbers providing amplitude and frequency information for each point in the time series. Instead of relying on subjective visual examination, we need to evaluate the most effective discriminants by making the required discriminant measurements within the spectrograms. Accurate measurements must be made of the sought-after patterns such as discrete Lg energy arrivals with decreasing frequency content and decreasing amplitudes.

For this purpose, we first normalized the Lg wavetrain from events at various recording distances so that the number of time windows used for spectrograms is the same for all events. Lg from seismic events at regional distances is known to have a fairly constant velocity of 3.5 km/sec. Coda waves arrive after the direct phase and are believed to be body waves scattered by randomly located crustal heterogeneities (Aki and Chouet, 1975). The term Lg coda generally refers to seismic arrivals at travel times greater than about twice the direct Lg (e.g., Hartse et al., 1995). Our selection of Lg wavetrain represents a time window starting at Lg (i.e., at velocity of about 3.5 km/sec) and ending at a travel time no greater than about twice the direct Lg time. In the future, we will refer to this Lg window as the Lg "wavetrain", since it does not contain any usual Lg "coda".

We tried to quantify the two features (i.e., decreasing frequency content and decreasing amplitudes with time) of the Lg wavetrain on spectrograms by first selecting the Lg wavetrain starting at a velocity of 3.3 km/sec (instead of 3.5 km/sec), because the scattered arrivals are expected to be somewhat delayed as compared to the direct Lg. The Lg wavetrain used for analysis was taken to be from t_1 to t_2 (= t_2-t_1), where t_1 = D/(3.3 km/sec) and t_2 = D/(1.65 km/sec). Thus, t_2-t_1=D/(3.3 km/sec). The moving time window, w for spectrograms was selected to be 1/10 of the selected Lg wavetrain, i.e., w = (t_2-t_1)/10 and the slice interval (time shift) was one-fourth of the moving window length. With these parameters, each spectrogram contained results from approximately 40 time windows within t_2-t_1

Several measurements on both explosion and earthquake spectrograms were made, but most of these did not look promising for source discrimination. However, the following measurement, which combines both temporal features (i.e., decreasing frequency and decreasing amplitudes) for explosions, provided encouraging results.

For each time slice, a mean weighted frequency, f(mean) is defined as

$$f(mean) = (f_1A_1 + f_2A_2 + f_3A_3 + \ldots..)/(A_1 + A_2 + A_3 + \ldots..) \quad (1)$$

where A_1, A_2, A_3, ... are the amplitudes associated with frequencies of f_1, f_2, f_3, ... The frequency range is generally selected to be 0.3 to 2.0 Hz, for which the short-period Rg is generally dominant.

When these f(mean) values are plotted versus time within t_1 and t_2, a series of peaks representing prominent low-frequency arrivals are observed. For explosions, the frequency values corresponding to these peaks may be expected to decrease more systematically than for earthquakes. A linear regression of these peak frequency values versus time should therefore indicate much smaller variance for explosions than for earthquakes. The above statement is of course based on several simplifying assumptions, including (i) a single dominant source of explosion Rg, (ii) several near-source discrete sources of scattering generate similar scattered S waves (i.e., similar scattering functions), and (iii) attenuation of Rg with distance is strong and not much dependent on epicenter-to-scatterer azimuthal direction. If these assumptions are valid, all prominent spectral peaks in the Lg wavetrain should be due to Rg-to-S arrivals, and they should progressively decrease with arrival time in both frequency content and amplitude. Most of the contribution to f(mean) for a given value of arrival time comes from the peak frequency and amplitude associated with the distinct Rg-to-S scattered arrival.

Our objective is to examine the variance associated with linear regression between f(mean) versus time based only on prominent large-amplitude arrivals. For this purpose, we need to (1) correct for the general decrease in wavetrain amplitude with time and (2) remove the influence of low-amplitude arrivals filling the gaps between adjacent spectral peaks. For (1), all spectral amplitudes within the 0.3-2.0 Hz frequency band and within the selected Lg wavetrain (i.e., from time t_1 to t_2) were plotted versus travel time, t. A linear regression is carried out and the mean slope, s is determined. This slope, s is almost always negative for both explosions and earthquakes because of attenuation with distance and time. In order to include the later arriving spectral peaks with generally lower amplitudes into our analysis, an attenuation with time correction was applied to all amplitude values by increasing the amplitudes at a given travel time, t by the positive amount $-s(t-t_1)$. In this way, the mean slope for the selected amplitude values became 0. In order to correct for (2), we retained only those amplitude points, which were within the top 25% values. These amplitude and associated frequency values are used for the linear regression in equation (1), and the corresponding standard deviation is determined. A correction for amplitude differences between various seismic events because of their magnitudes is applied by using normalized standard deviation values based on division by the average value of all mean weighted frequency values within t_2-t_1.

4.1 Application to NTS Explosions and Nearby Earthquakes

We carried out the above analysis on ten Yucca Flat explosions and ten nearby earthquakes recorded at the LLNL station, MNV (Table 1 and Figure 1). As examples, spectrograms and linear regression results from the Yucca Flat explosion, Starwort (26 April 1973) and the Massachusetts Mountain earthquake (5 August 1971), both recorded at MNV, are shown in Figures 2 through 5. The Lg wavetrain on the Starwort spectrogram (Figure 2) shows several prominent peaks with progressively decreasing frequency content, combined with generally decreasing amplitudes. On the other hand, the spectral peaks on the earthquake spectrogram (Figure 4) indicate significantly different characteristics. The linear regression plots of f(mean) versus travel time for the Lg wavetrain for the two events (Figures 3 and 5) indicate significant difference in their normalized standard deviation values. The results for all 20 events are shown in Figure 6. The mean value for the earthquake population is about 55% higher than for the

explosion population. Considering that results from only one recording station are shown, it seems that the observed differences in normalized standard deviation values should be useful for source discrimination.

TABLE 1. 10 NTS Explosions and 10 Nearby Earthquakes Used in Study

No.	Date	Name	Depth	Distance
			(m)	(km)
1	19730426	STARWORT	564	235
2	19780223	REBLOCHON	658	235
3	19790906	HEARTS	640	238
4	19790908	PERA	200	234
5	19810115	BASEBALL	564	238
6	19810716	PINEAU	204	240
7	19811112	ROUSANNE	518	237
8	19840802	CORREO	335	246
9	19881013	DALHART	640	238
10	19891115	MULESHOE	244	239
			(km)	(km)
11	19710805	MMEQ	4.00	254
12	19801025	OCT2580	5.00	179
13	19820512	MAY1282	10.00	300
14	19830604	JUN0483	6.00	283
15	19920629	LITTLESKULL_A	7.00	253
16	19920705	LITTLESKULL_B	7.00	253
17	19920913	LITTLESKULL_C	9.68	250
18	19920914	LITTLESKULL_136	8.70	251
19	19921008	LITTLESKULL_140	10.20	249
20	19930530	ROCKVALLEY	10.43	252

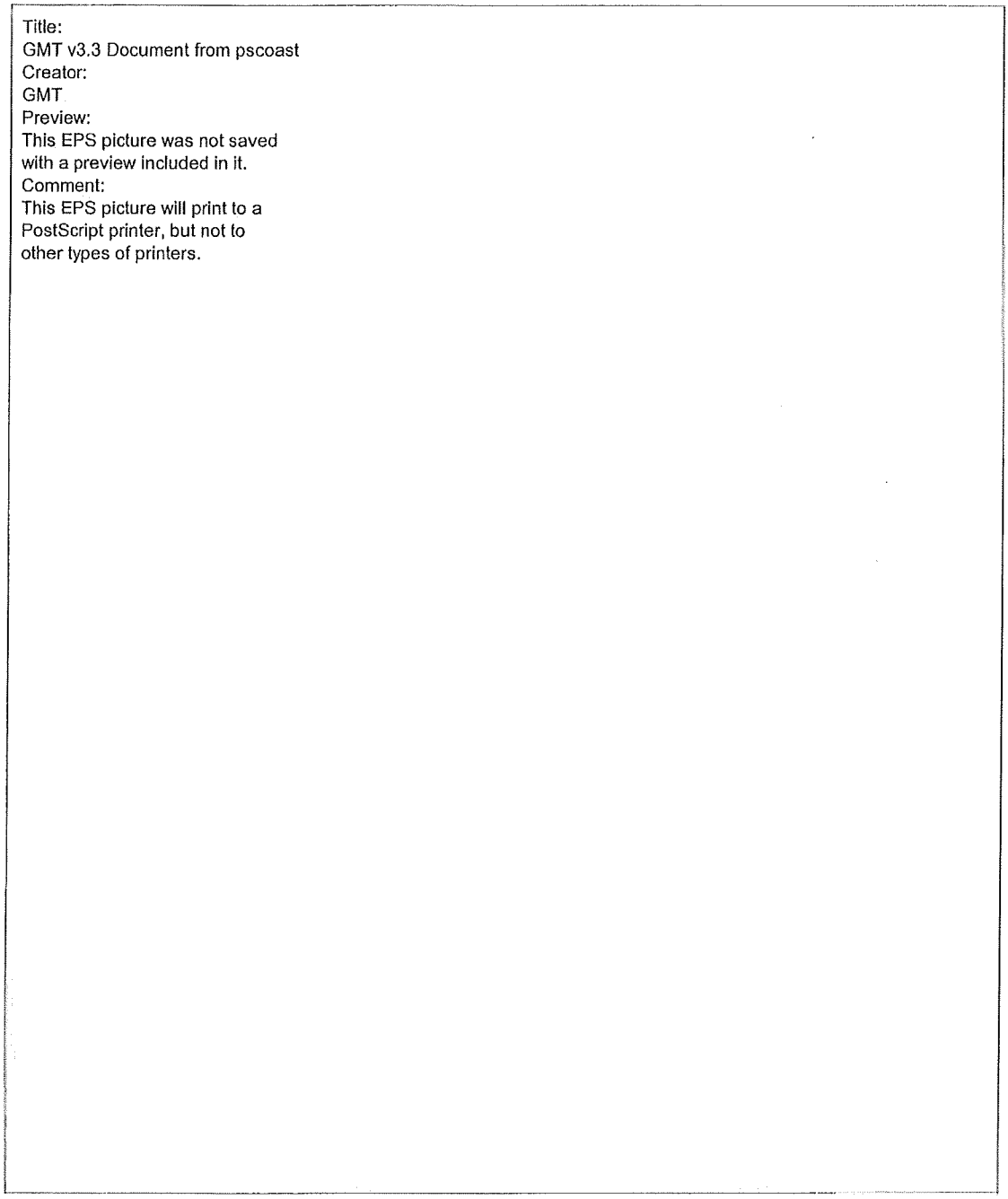

Figure 1. Location map of 10 Yucca Flat explosions (red) and 10 nearby earthquakes (black circles) recorded at the LLNL station, MNV located approximately along the north-west direction. The explosions cover a wide range of shot depths (200 to 658 m) and several are located close to each other.

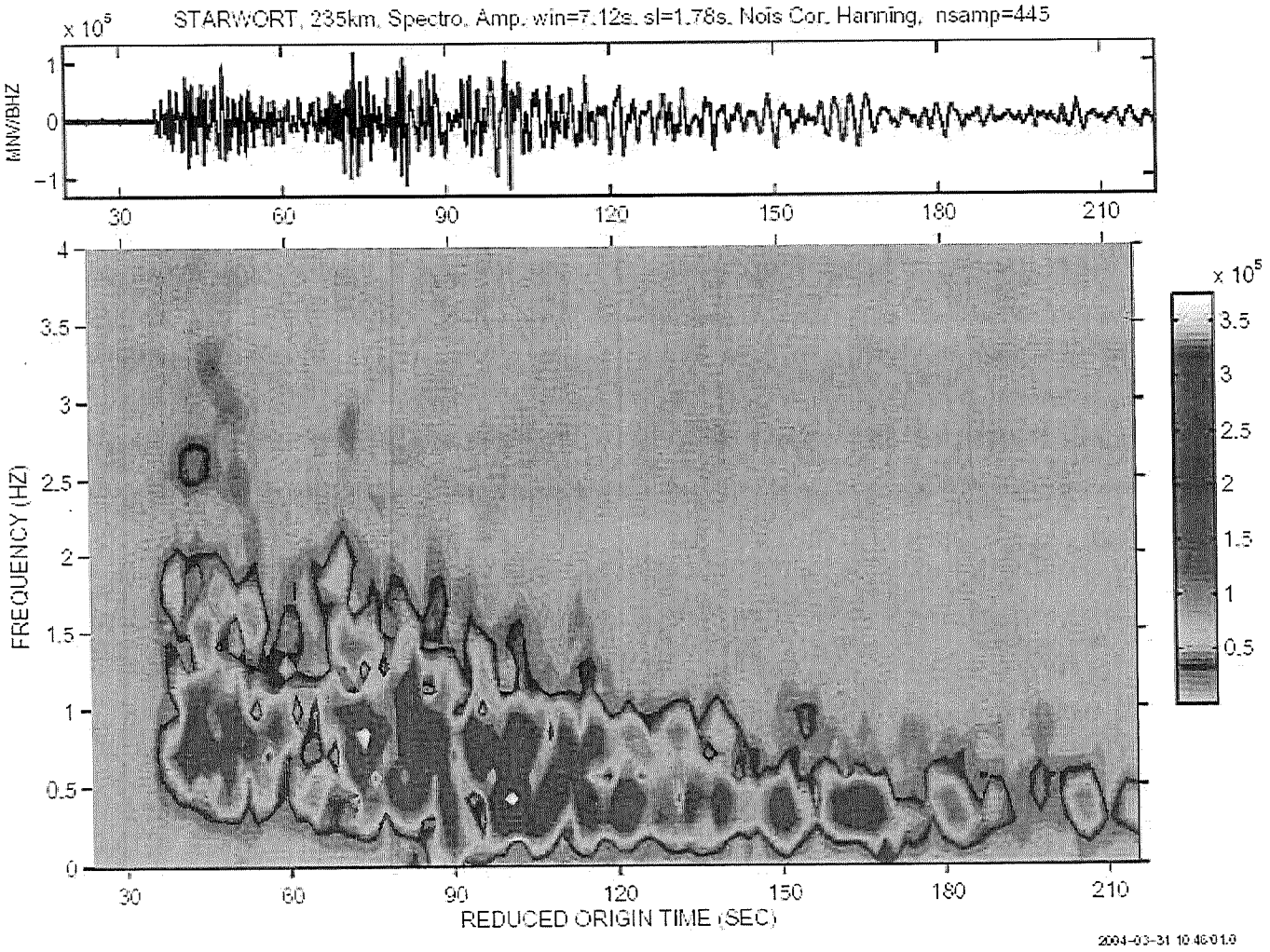

Figure 2. Spectrogram of Starwort recorded at MNV. The Lg wavetrain, starting at about 71 sec, shows several prominent peaks with progressively decreasing frequency content and amplitude.

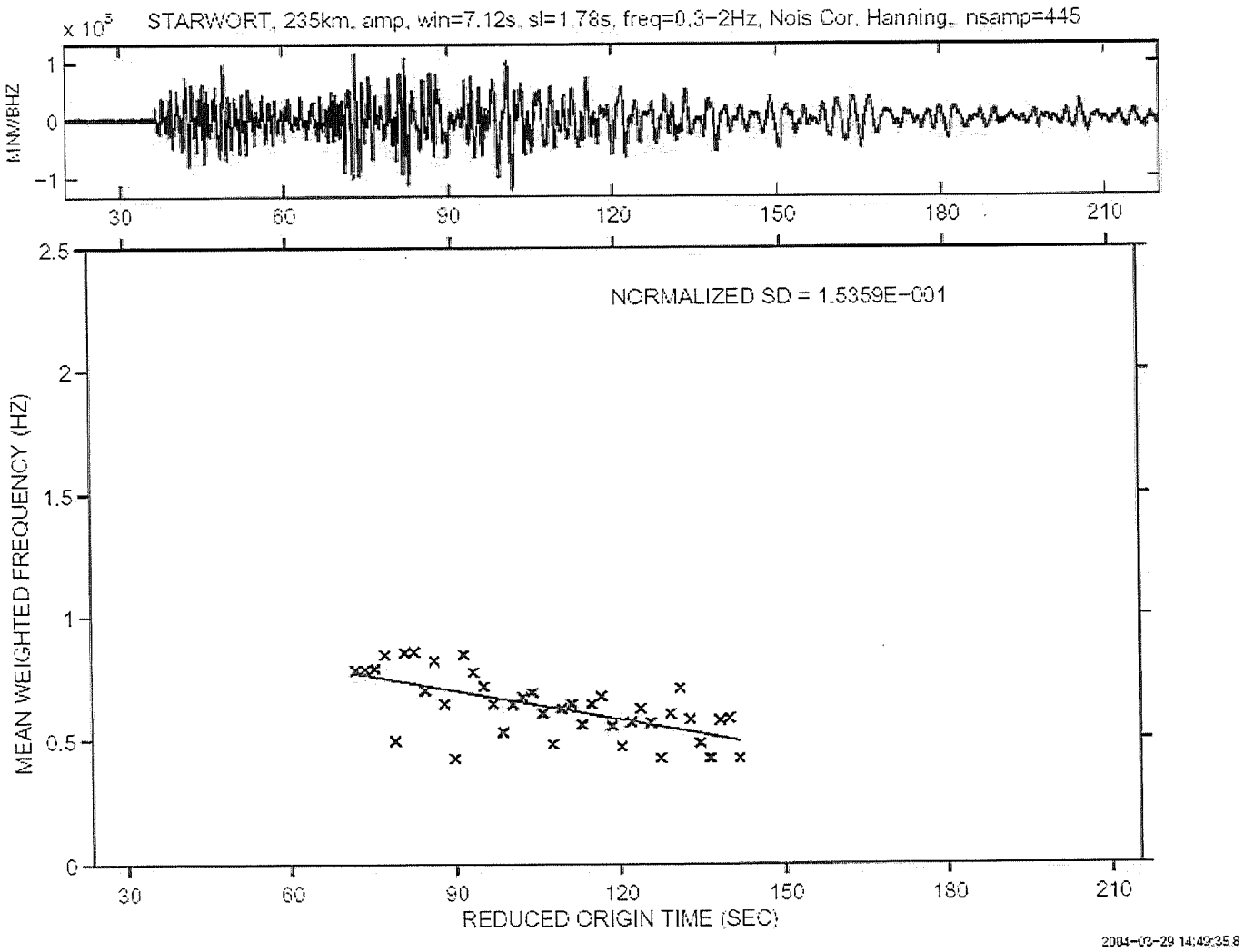

Figure 3. Mean weighted frequency versus travel time, within the time window D/(3.3 km/sec) and D/(1.65 km/sec), where D is the epicentral distance for Starwort recorded at MNV. Linear regression (red line) and the associated normalized standard deviation are indicated.

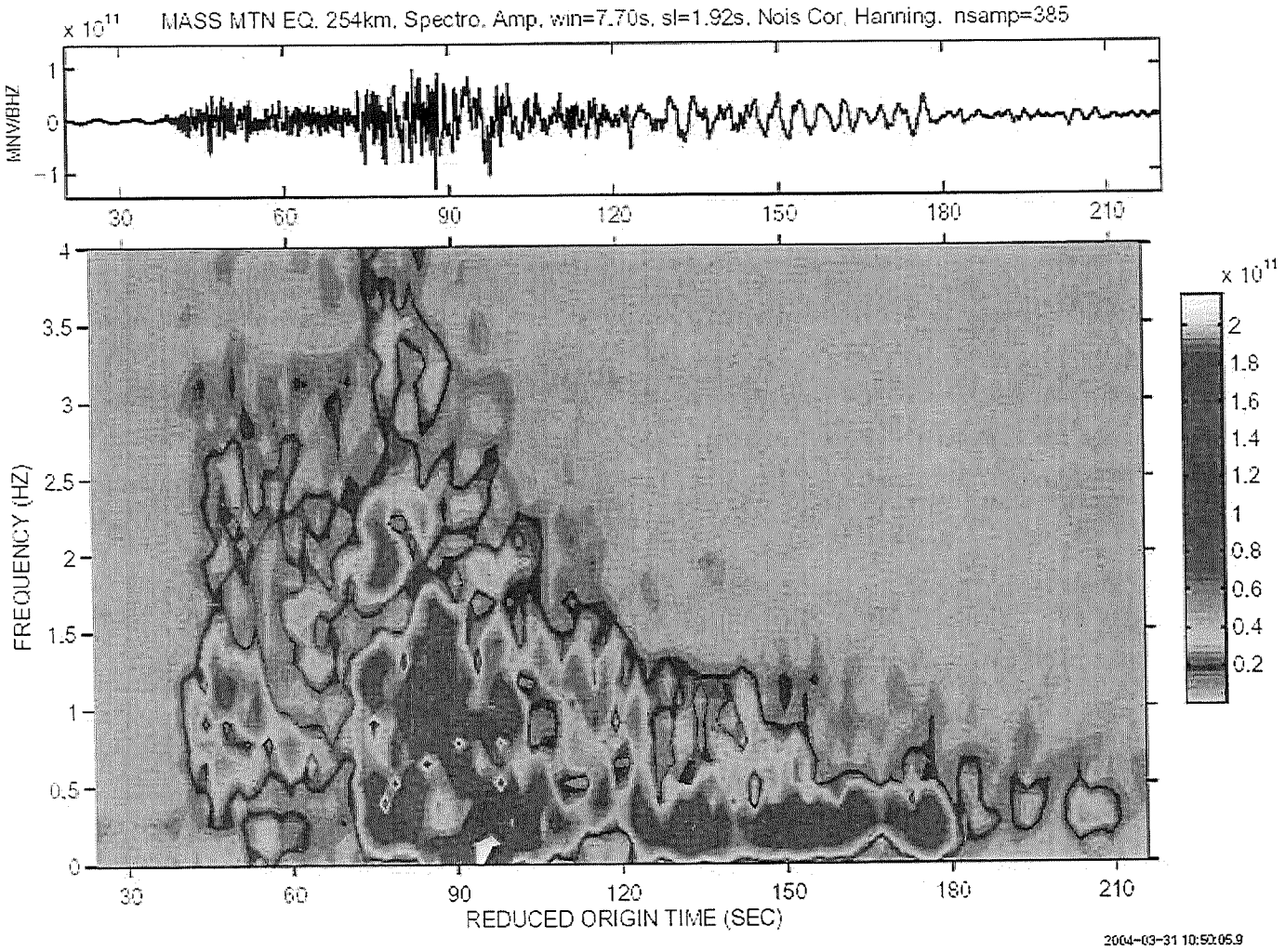

Figure 4. Spectrogram of the Massachusetts Mountain earthquake recorded at MNV. The Lg wavetrain, starting at about 77 sec, shows several prominent peaks but these peaks are not as systematically decreasing in frequency content and amplitude as those for the explosion in Figure 2.

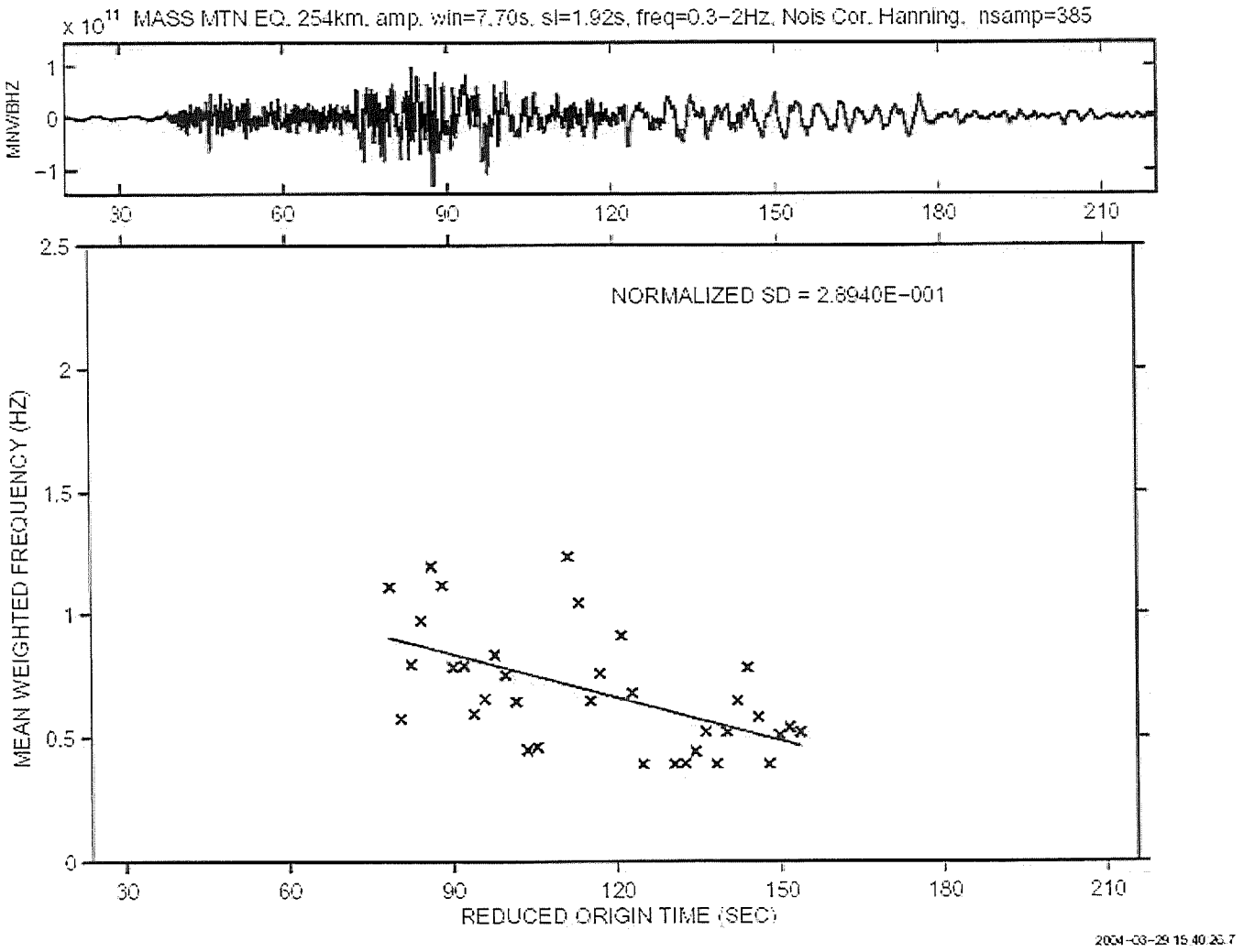

Figure 5. Mean weighted frequency versus travel time, within the time window D/(3.3 km/sec) and D/(1.65 km/sec), for the Massachusetts Mountain earthquake recorded at MNV. Linear regression (red line) and the associated normalized standard deviation are indicated.

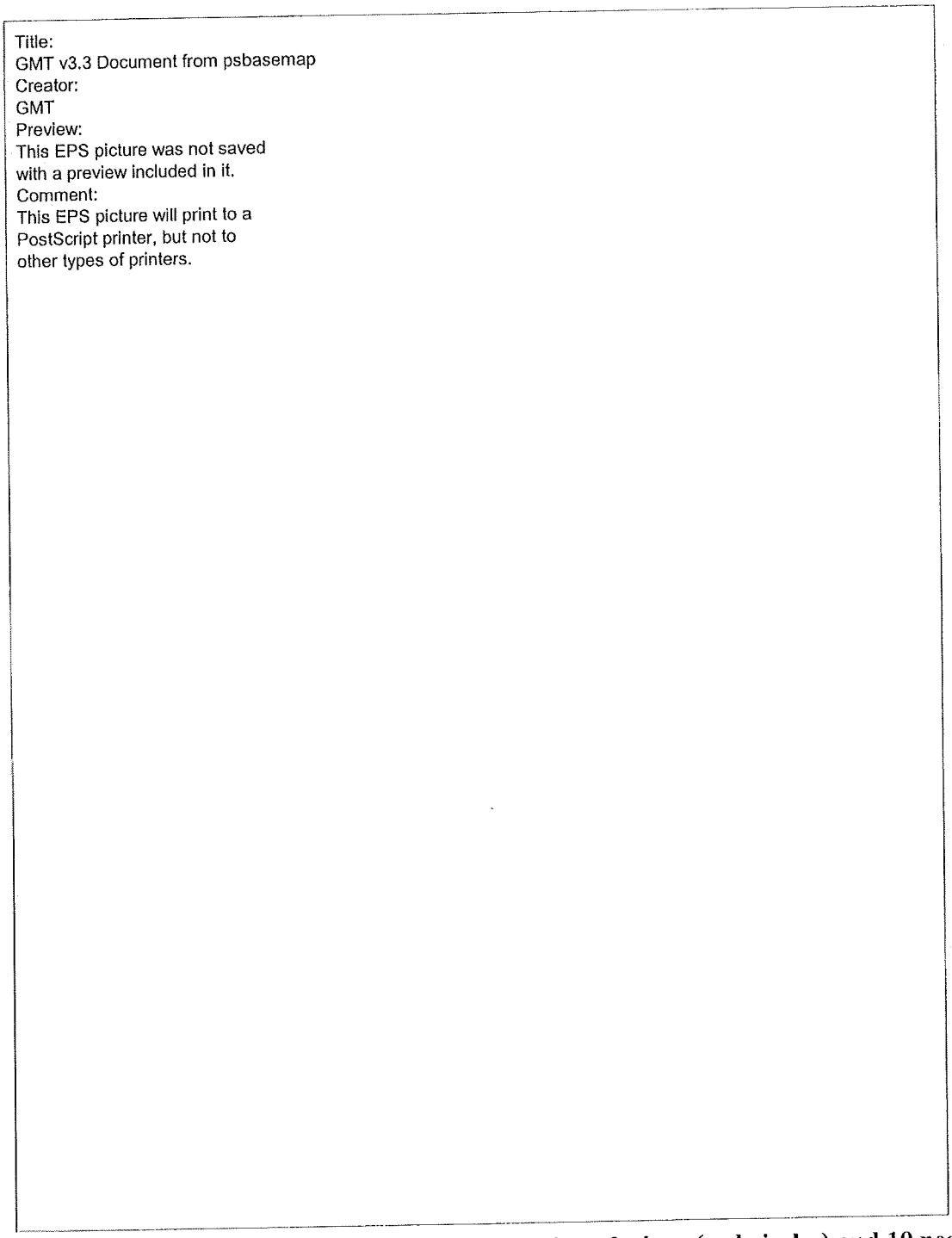

Figure 6. Normalized standard deviation for 10 NTS explosions (red circles) and 10 nearby earthquakes (black circles) recorded at MNV. The earthquake and explosion populations are fairly well separated. The mean value for the earthquake population is about 55% higher than for the explosion population, suggesting that differences in standard deviation values should be useful for source discrimination.

4.2 Results from KTS Explosions and Nearby Earthquakes

We carried out analysis similar to that for the U.S. events using 10 Kazakh Test Site (KTS) explosions and 10 earthquakes (Table 2 and Figure 7). However, because of the much larger epicentral distances, the Lg wavetrain used for analysis was considered to be the interval within group velocities of 3.4 and (2/3)X3.4=2.27 km/sec. Thus t2-t1= D/(2.27)-D/(3.4)=D/(6.8 km/sec). The moving time window, w for spectrograms was selected to be 1/20 of t2-t1 and the slice interval was one-half of the moving window length. With these parameters, each spectrogram contained results from approximately 40 time windows within t2-t1, the same number as for the U.S. data.

Example spectrograms and linear regression results from an explosion and an earthquake, both recorded at the broadband digital station WMQ, are shown in Figures 8 through 11. Similar to the spectrograms for NTS explosions, the Lg wavetrain on the explosion spectrogram in Figure 8 shows several prominent peaks with progressively decreasing frequency content with generally decreasing amplitudes. In comparison, the spectral peaks on the earthquake spectrogram in Figure 10 indicate significantly different characteristics. The linear regression plots of f(mean) versus travel time for the Lg wavetrain for the two events (Figures 9 and 11) indicate significant difference in their normalized standard deviation values. The results for all 20 events are shown in Figure 12; the mean value for the earthquake population is about 52% higher than that for the explosion population. These results, similar to those for the U.S. data (Figure 6), suggest that observed differences in the normalized standard deviation values can be useful for source discrimination based on the use of only Lg. It should be noted that, unlike the U.S. events (Figure 1), the available earthquakes are at significantly different locations as compared to the explosions, which are clustered together. This means that the differences in propagation paths and source-receiver distances for the two types of events are likely to influence significantly the source discrimination results; much more than for the U.S. data. This provides a possible explanation for the Soviet discrimination results (Figure 12) to be not as satisfactory as for the U.S. events (Figure 6).

5. Discrimination Based on Lg Spectral Ratios and Spectral Slopes

Several investigators (e.g., Taylor et al., 1988; Gupta and Wagner, 1998) have used Lg spectral ratios for regional discrimination with limited success. There have also been a few studies of spectral slope as a discriminant but with ambiguous results. For example, by analyzing high frequency data, Chael (1988) found the spectral slope of Pg to be a good discriminant for NTS explosions and southwestern earthquakes. Gupta and Wagner (1998) were probably the first to successfully use the spectral slope of Sg and Lg as a source discriminant.

5.1 Results from NTS Explosions and Nearby Earthquakes

By using the same dataset of ten NTS explosions and ten U.S. earthquakes (Table 1 and Figure 1), we obtained spectra of Lg wavetrain starting at a velocity of 3.5 km/sec. Multi-tapered spectra, corrected for noise, for 25.6 sec long windows were used to obtain mean log amplitudes within several frequency bands. Results for Lg(0.5-2 Hz)/(3-7 Hz) are shown in Figure 13 (open symbols). All ten explosions are at nearly the same distance (within 234 to 246 km), whereas the epicentral distances for earthquakes vary from 179 to 300 km. A source-receiver distance correction was therefore computed by assuming linear dependence with distance for the ten earthquake spectral ratios, as by Taylor et al. (1988). Normalizing all data to the mean distance of the ten explosions (i.e., 238 km), the corrected results for all 20 events are also shown in

Figure 13 (filled symbols), in which the mean values for the explosion and earthquake populations differ by 0.69 log units. The mean spectral slopes over the frequency range of 0.5 to 7.0 Hz for all events are shown in Figure 14, which shows results for both without and with distance correction. The explosion and earthquake populations are well separated (about 0.19 log units). Considering that results in Figures 13 and 14 are from only one recording station, it seems that the observed differences in the Lg spectral ratios and spectral slopes may serve as powerful regional discriminants based only on the use of Lg.

Table 2. 10 Shagan Explosions and 10 Earthquakes Used in Study

No.	Date	Origin Time	Lat	Lon	Depth	Distance	mb
					(km)	(km)	
1	19870620	00:53:07.16	49.9353	78.7440	0.0	962	6.1
2	19870802	00:58:09.27	49.8806	78.8745	0.0	951	5.9
3	19871213	03:21:07.25	49.9632	78.7929	0.0	961	6.1
4	19880213	03:05:08.28	49.9367	78.8637	0.0	956	6.0
5	19880403	01:33:08.21	49.9083	78.9081	0.0	951	6.0
6	19880504	00:57:09.15	49.9495	78.7501	0.0	963	6.1
7	19880914	03:59:59.77	49.8779	78.8229	0.0	954	6.0
8	19881112	03:30:06.27	50.0431	78.9688	0.0	958	5.4
9	19881217	04:18:09.24	49.8820	78.9245	0.0	948	5.8
10	19891019	09:49:59.90	49.9223	78.9081	0.0	952	5.9
11	19920225	09:30:51.90	43.2700	78.1200	11.0	776	4.5
12	19920625	09:41:49.80	40.5600	78.4500	33.0	844	4.6
13	19930213	10:34:28.70	38.7600	78.1600	28.0	975	4.5
14	19930223	15:20:29.80	47.9600	86.1200	23.0	476	4.4
15	19930303	03:24:26.00	40.5000	78.9300	28.0	812	4.5
16	19931201	14:54:48.90	44.9700	93.8300	15.0	505	4.6
17	19931230	14:24:06.40	44.8000	78.8000	31.0	718	5.6
18	19940509	09:14:10.50	40.3500	79.0600	24.0	811	4.9
19	19950528	21:46:54.90	47.6700	85.5100	25.0	460	4.7
20	19951101	12:29:27.20	43.0100	80.2800	27.0	607	5.3

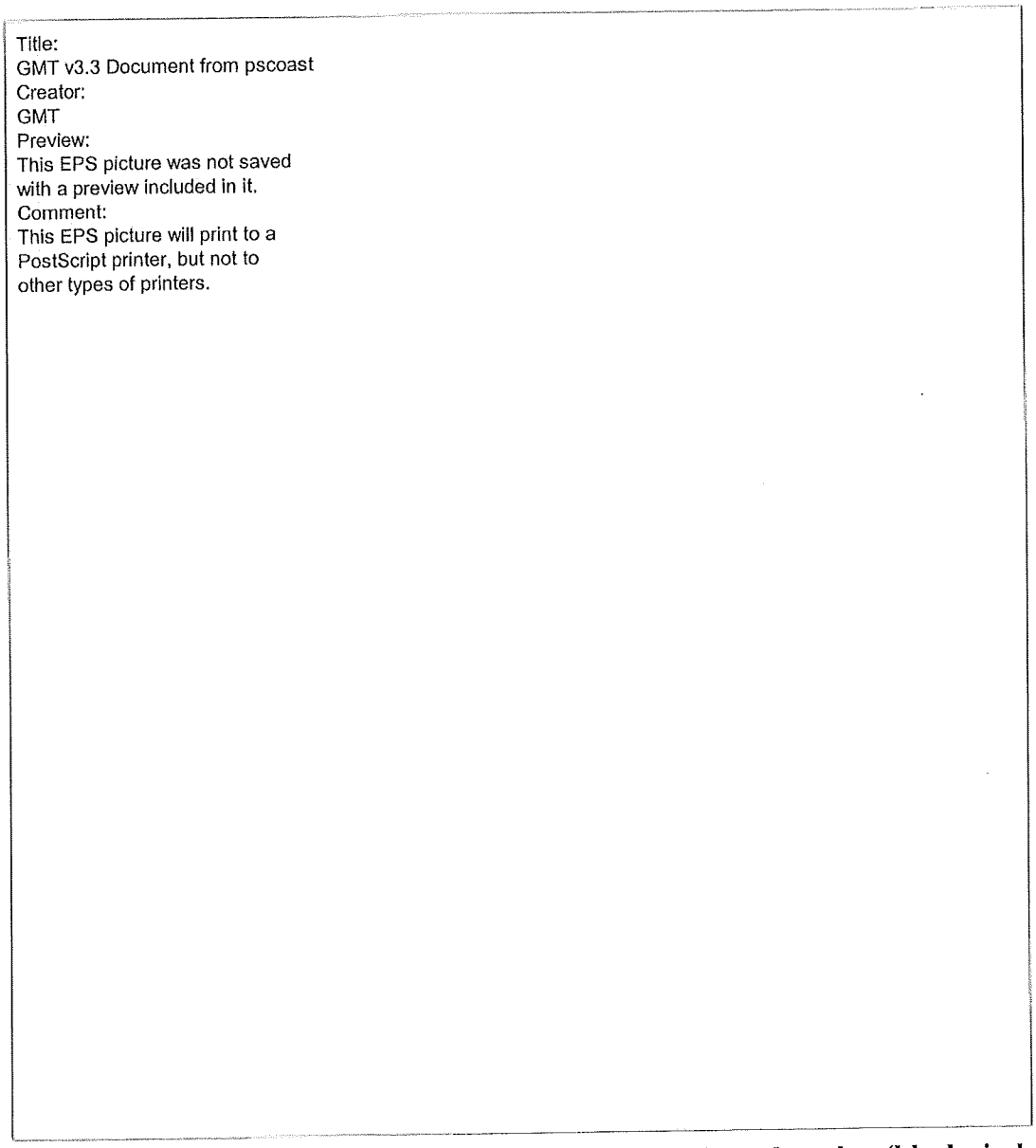

Figure 7. Location map of 10 KTS explosions (red) and 10 earthquakes (black circles) recorded at WMQ. Note that the available earthquakes are at significantly different locations as compared to the explosions which are clustered together.

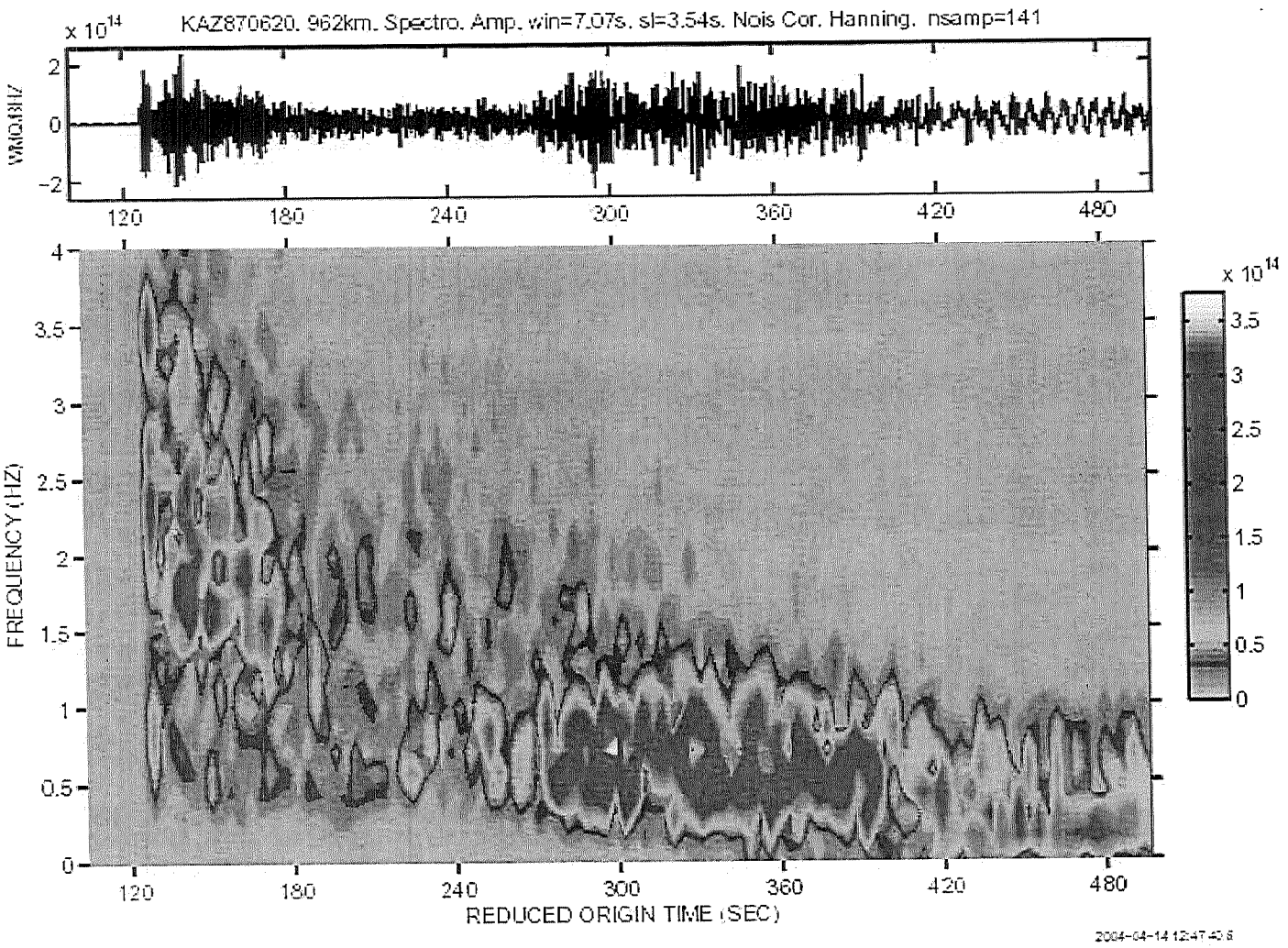

Figure 8. Spectrogram of KTS explosion of 20 June 1987 recorded at WMQ. The Lg wavetrain, starting at about 275 sec, shows several prominent peaks with progressively decreasing frequency content and amplitude.

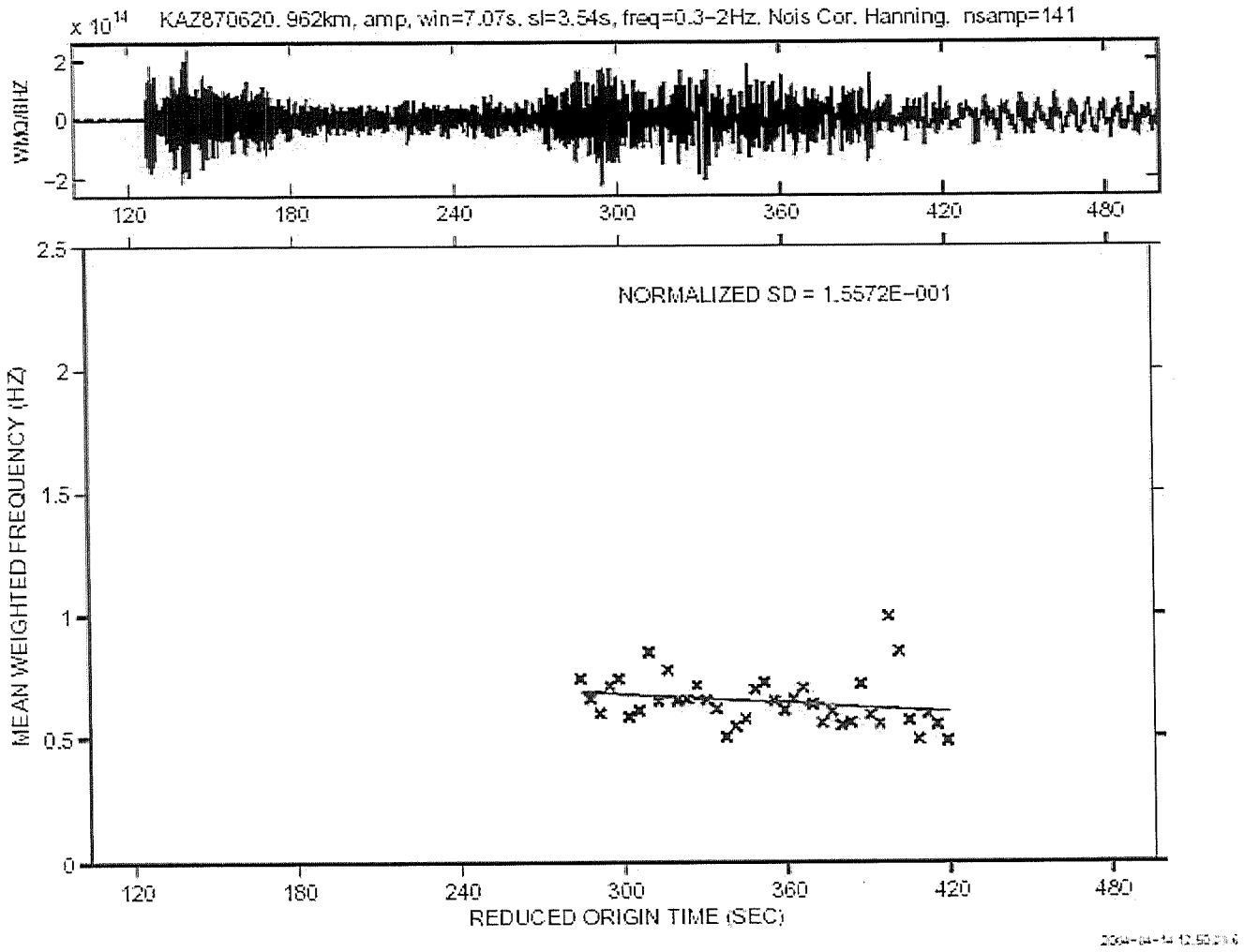

Figure 9. Mean weighted frequency versus travel time, within the time window D/(3.4 km/sec) and D/(2.27 km/sec), where D is the epicentral distance for the KTS explosion of 20 June 1987 recorded at WMQ. Linear regression (red line) and the associated normalized standard deviation are indicated.

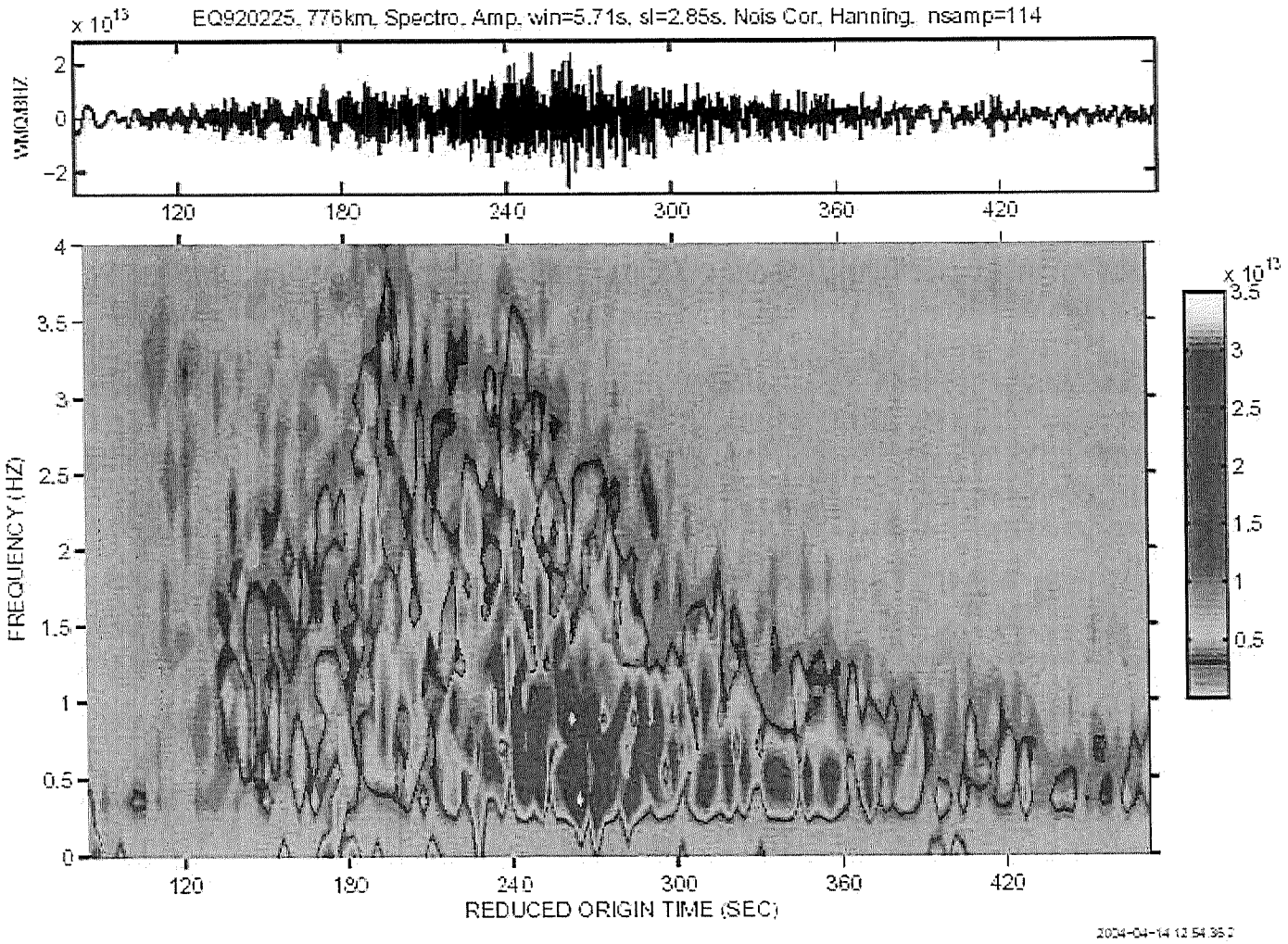

Figure 10. Spectrogram of the earthquake of 25 February 1992 recorded at WMQ. The Lg wavetrain, starting at about 222 sec, shows several prominent peaks but these peaks are not as systematically decreasing in frequency content and amplitude as those for the explosion in Figure 8.

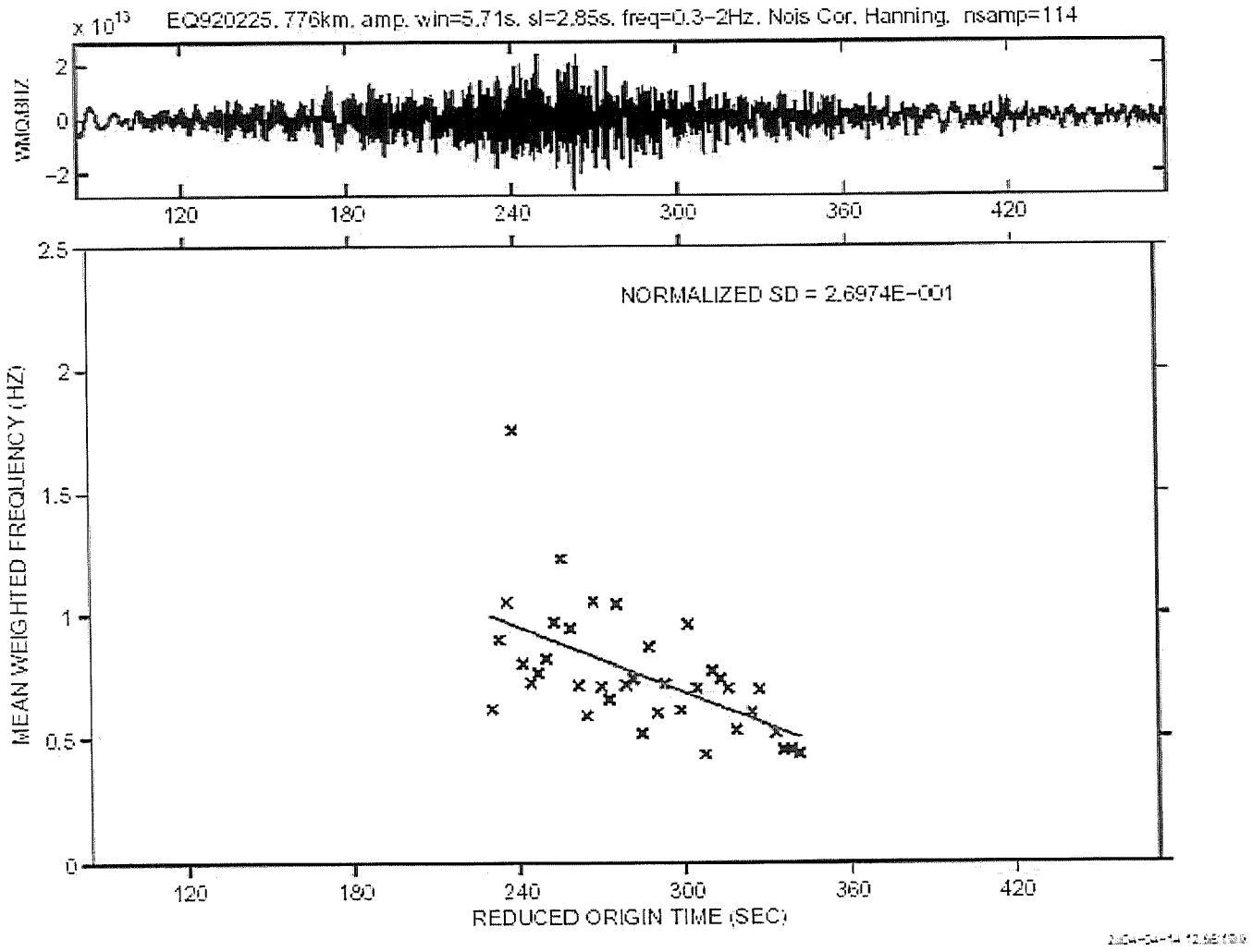

Figure 11. Mean weighted frequency versus travel time, within the time window D/(3.4 km/sec) and D/(2.27 km/sec), where D is the epicentral distance for the earthquake of 25 February 1992 recorded at WMQ. Linear regression (red line) and the associated normalized standard deviation are indicated.

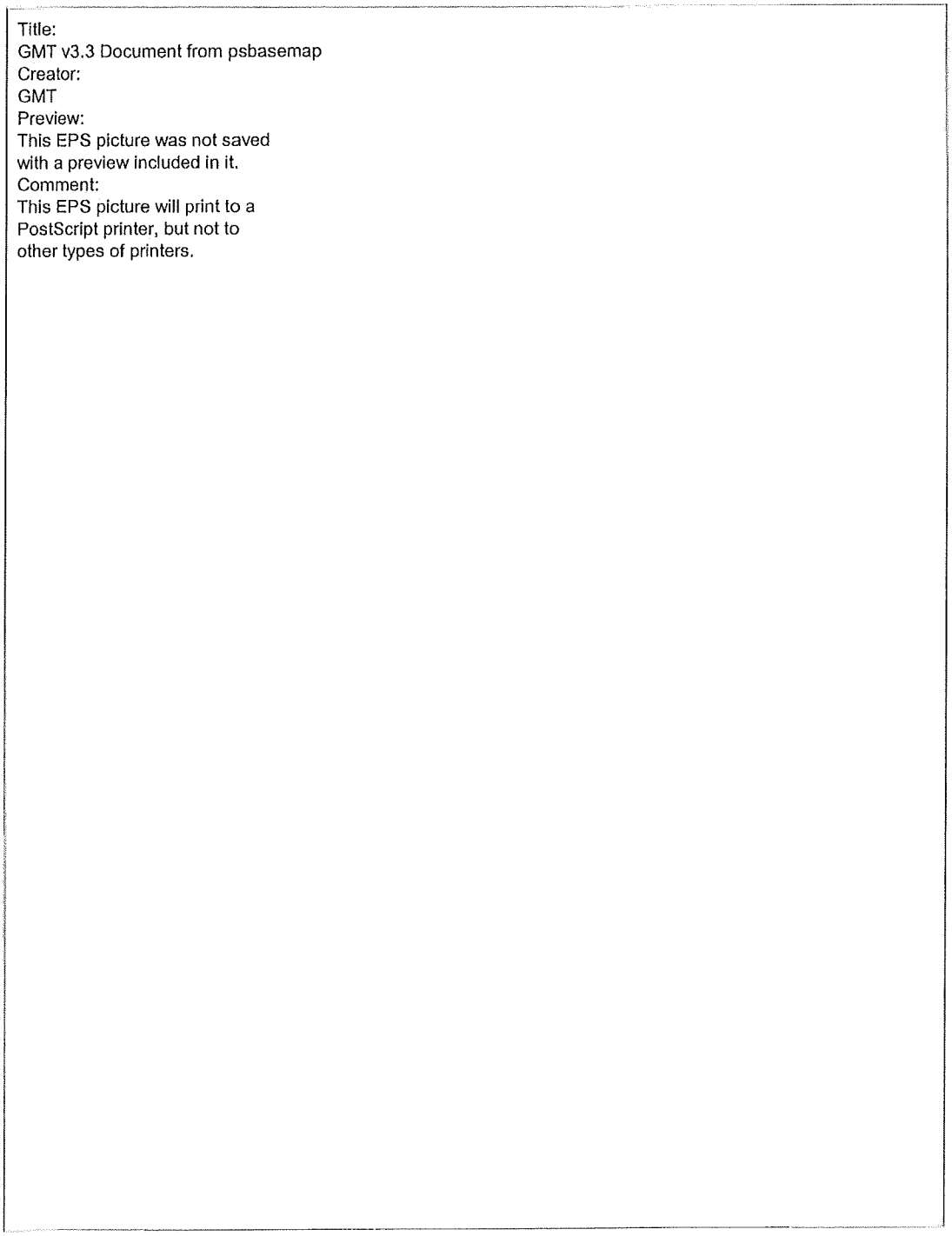

Figure 12. Normalized standard deviation for 10 KTS explosions (red circles) and 10 earthquakes (black circles) recorded at WMQ. The earthquake and explosion populations are separated such that the mean value for the earthquake population is about 52% higher than for the explosion population. Considering large differences in propagation paths to WMQ, these results should be useful for source discrimination.

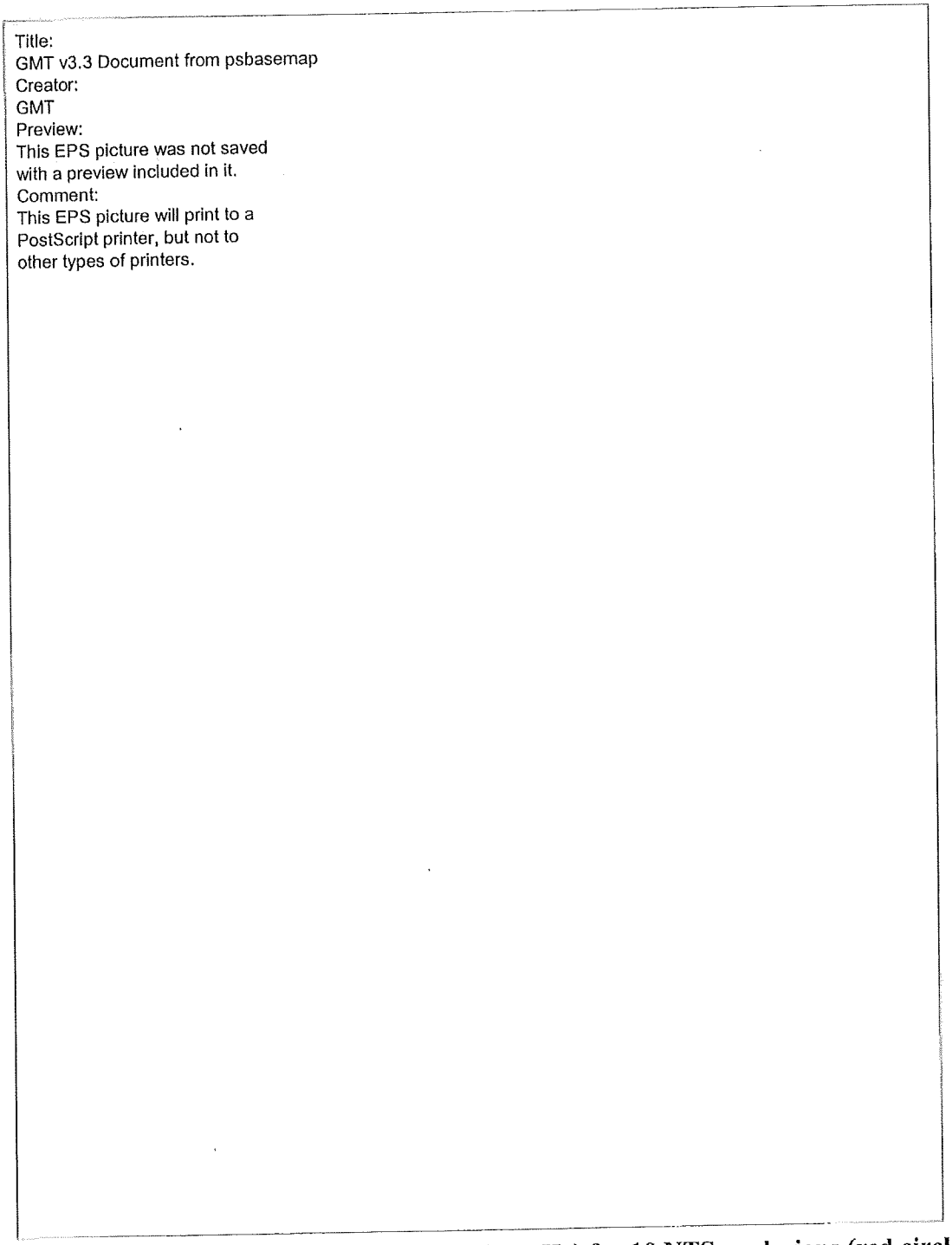

Figure 13. Mean spectral ratio Lg(0.5-2 Hz)/(3-7 Hz) for 10 NTS explosions (red circles) and 10 nearby earthquakes (black circles) recorded at MNV. Results without (open symbols) and with distance correction (filled symbols) are shown; the latter shows the earthquake and explosion populations to be well separated by 0.69 log units. Differences in Lg spectral ratios are therefore useful for source discrimination.

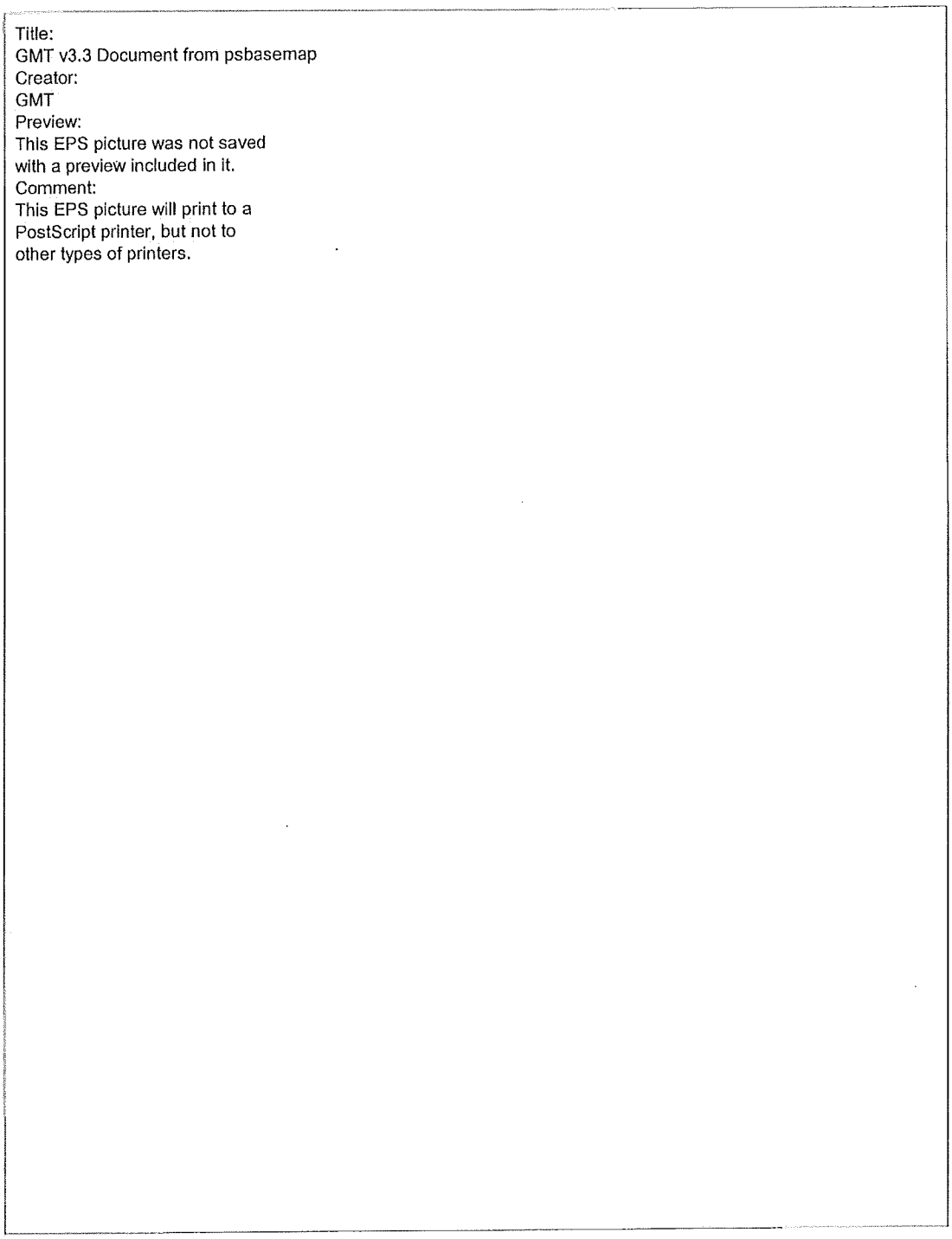

Figure 14. Mean spectral slope of Lg over 0.5-7.0 Hz for 10 NTS explosions (red circles) and 10 nearby earthquakes (black circles) recorded at MNV. Results without (open symbols) and with distance correction (filled symbols) are shown; the latter shows the earthquake and explosion populations to be well separated by 0.19 log units. Differences in Lg spectral slopes are therefore useful for source discrimination.

5.2 Results from KTS Explosions and Nearby Earthquakes

We used the same dataset of ten KTS explosions and ten earthquakes recorded at WMQ as used earlier (Table 2 and Figure 7) and obtained Lg spectra of 25.6 sec long windows by following the same procedure as for the U.S. data. As for the NTS shots, all ten explosions are at nearly the same distance (within 948 to 963 km). However, the epicentral distances for earthquakes vary from 476 to 975 km. Results for Lg(0.5-2 Hz)/(3-5 Hz), both without and with distance correction, are shown in Figure 15, after normalizing all data to the mean distance of the ten explosions (about 956 km). The explosion and earthquake populations, with their mean values differing by 0.41 log units, are fairly well separated. The mean spectral slopes over the frequency range of 0.5 to 5.0 Hz for all events are shown in Figure 16, which also shows results for cases both without and with distance correction. The explosion and earthquake populations are well separated (about 0.15 log units). Considering that results in Figures 15 and 16 are also from only one recording station, it seems that the observed differences in the Lg spectral ratios and spectral slopes may serve as powerful regional discriminants, similar to the findings for the U.S. data. It is also interesting to note that, although the available Soviet earthquakes are at significantly different locations as compared to the explosions (unlike the U.S. events), the Lg spectral ratios and spectral slopes are still as effective regional discriminants as for the U.S. data.

6. Discrimination Based on Skewness and Kurtosis of Lg Spectra

A recent study by Ortiz et al. (2002) found statistical measures such as skewness and kurtosis to be useful for source discrimination at regional distances. Their approach, based on the use of time-series analysis of various regional phases, provided effective discrimination between nuclear explosions and earthquakes. We modified their procedure to frequency domain measurements and applied it to the spectra of Lg from both types of seismic events recorded at a common station.

Following Ortiz et al. (2002), skewness for signal S(t) may be expressed as

$$W(t) = \frac{\sum_i (t_i - t_0)^3 |S(t_i)|}{\left[\sum_i (t_i - t_0)^2 |S(t_i)|\right]^{3/2}} \qquad (1)$$

We used the following similar frequency-domain relationship for skewness

$$W(f) = \frac{\sum_i (f_i - f_0)^3 A_i}{\left[\sum_i (f_i - f_0)^2 A_i\right]^{3/2}} \qquad (2)$$

and for kurtosis

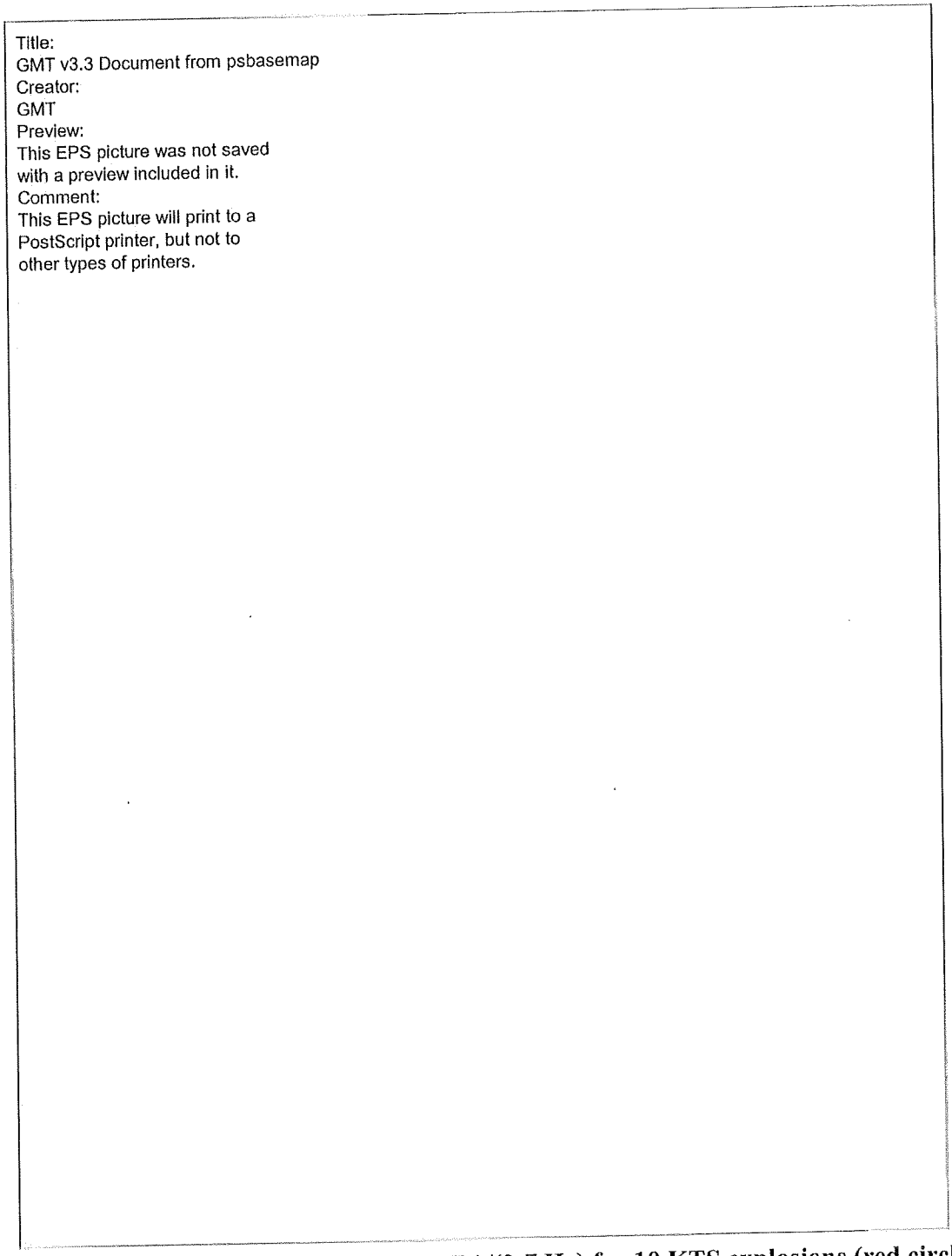

Figure 15. Mean spectral ratio Lg(0.5-2 Hz)/(3-7 Hz) for 10 KTS explosions (red circles) and 10 earthquakes (black circles) recorded at WMQ. Results without (open symbols) and with distance correction (filled symbols) are shown; the latter shows the earthquake and explosion populations to be well separated by 0.41 log units. Differences in Lg spectral ratios are therefore useful for source discrimination.

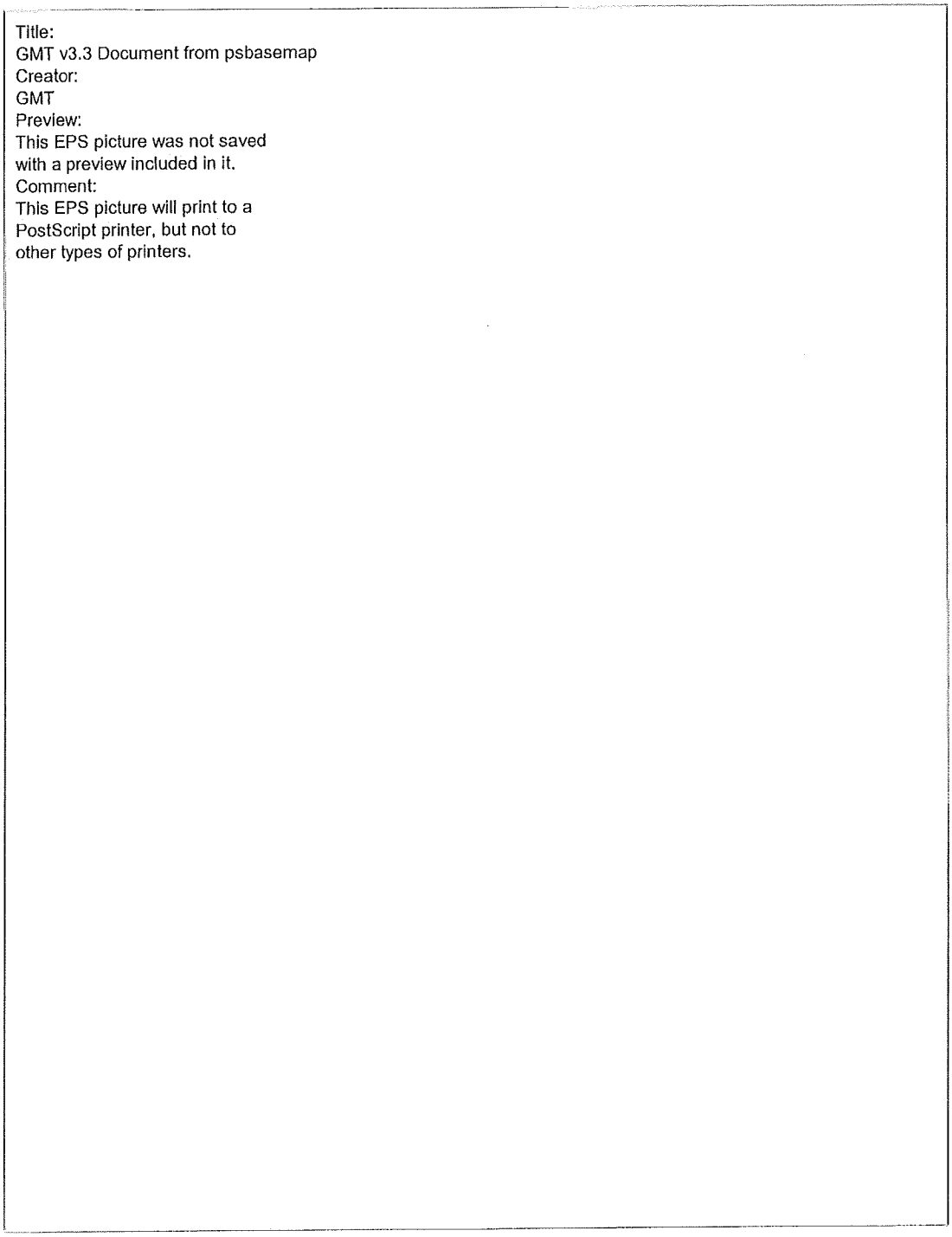

Figure 16. Mean spectral slope of Lg over 0.5-7.0 Hz for 10 KTS explosions (red circles) and 10 earthquakes (black circles) recorded at WMQ. Results without (open symbols) and with distance correction (filled symbols) are shown; the latter shows the earthquake and explosion populations to be well separated by 0.15 log units. Differences in Lg spectral slopes are therefore useful for source discrimination.

$$K(f) = \frac{\sum_i (f_i - f_0)^4 A_i}{\left[\sum (f_i - f_0)^2 A_i\right]^2} \qquad (3)$$

The above two relationships provide results which vary with the absolute value of the amplitudes, A_i which, in this study, are in log units. In order to obtain results that only depend on the shape of the spectra (rather than absolute values), all mean amplitudes within a specified frequency range are scaled by assigning the same fixed value for all events. This required all A_i values (in log units) for a given event to be adjusted by the same normalizing amount, which was of course different for different events.

6.1 Application to NTS Explosions and Nearby Earthquakes

Lg spectra for 25.6 sec long Lg windows, corrected for noise, were obtained for all 20 seismic events recorded at MNV. For the frequency range of 0.5-7.0 Hz, skewness and kurtosis were computed by using equations (2) and (3). Mean values of A_i for 0.5-7.0 Hz for most events were close to 3 so that a normalizing amount of 3.0 was used for all 20 events. Actually, skewness based on the use of equation (2) yielded negative values for all 20 seismic events and Figure 17 shows the absolute (positive) values. The explosion and earthquake populations are remarkably well separated. However, the results for kurtosis showed no significant discrimination between the two types of seismic events. A source-receiver distance correction was applied to the skewness and the results are also included in Figure 17. Furthermore, we also derived the skewness and kurtosis by using a normalizing amount of 5.0, but the results remained almost the same; indicating that the choice of the normalizing amount is not important. Considering that the skewness results in Figure 17 are from only one recording station, it seems that the observed differences in the skewness of Lg spectra serve as an effective regional discriminant.

6.2 Results from KTS Explosions and Nearby Earthquakes

As for the U.S. data, Lg spectra for 25.6 sec long Lg windows, corrected for noise, were obtained for all 20 seismic events recorded at WMQ. For most events, mean values of A_i for 0.5-5.0 Hz were close to 3 so that a normalizing amount of 3.0 was used for all 20 events. As for the NTS data, skewness based on the use of equation (2) yielded negative values for all 20 seismic events and Figure 18 shows the absolute (positive) values. The explosion and earthquake populations are well separated. However, the results for kurtosis showed no significant discrimination between the two types of seismic events. A source-receiver distance correction was applied to the skewness and the results are also included in Figure 18. Considering that the skewness results in Figure 18 are from only one recording station, it seems that the observed differences in the skewness of Lg spectra serve as an additional regional discriminant, similar to the result for U.S. explosion and earthquake data (Figure 17).

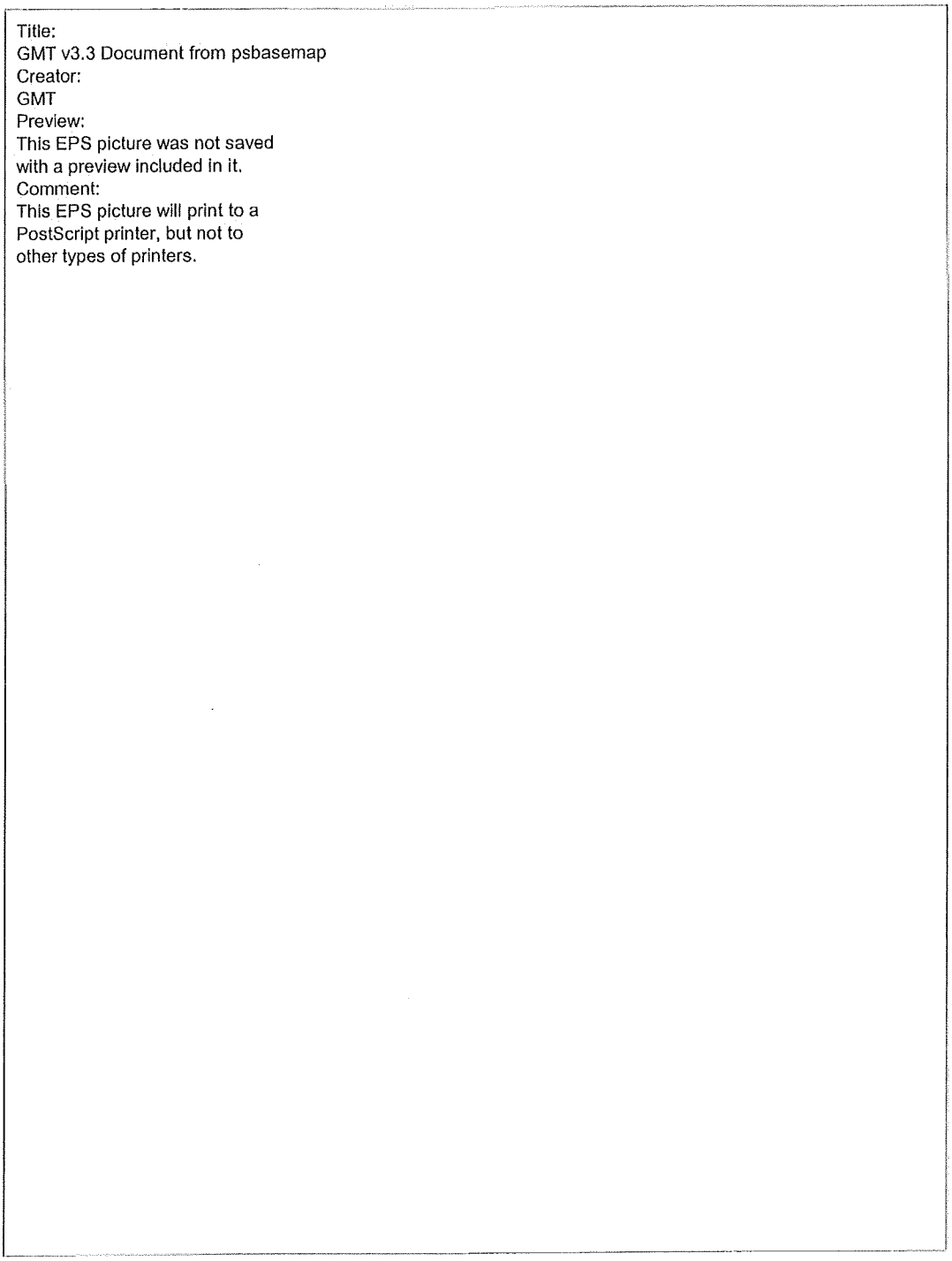

Figure 17. Skewness for the frequency range of 0.5-7.0 Hz for 10 NTS explosions (red circles) and 10 nearby earthquakes (black circles) recorded at MNV. Results without (open symbols) and with distance correction (filled symbols) are shown; the latter shows the earthquake and explosion populations to be well separated. Differences in skewness are therefore useful for source discrimination.

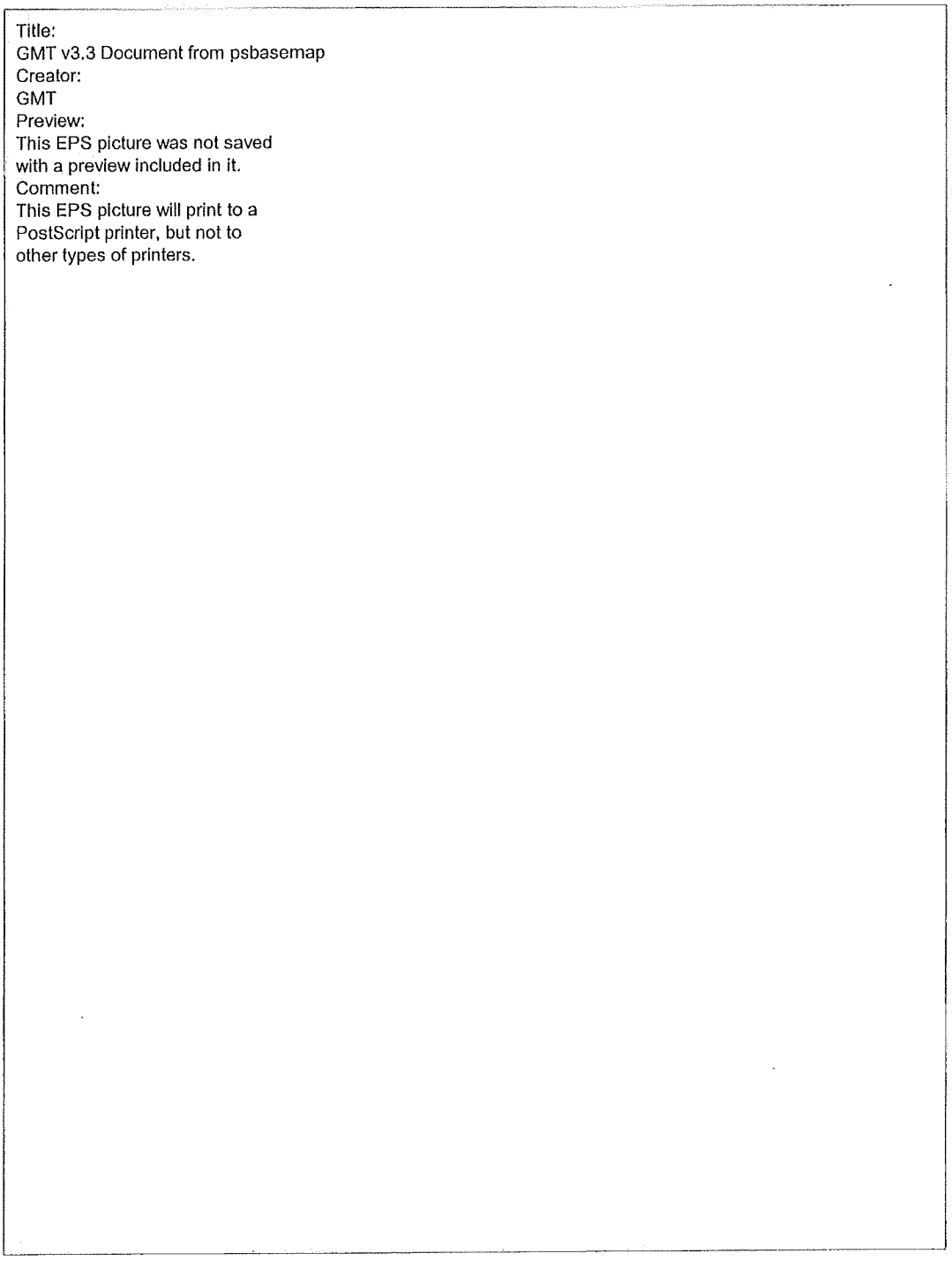

Figure 18. Skewness for the frequency range of 0.5-5.0 Hz for 10 KTS explosions (red circles) and 10 nearby earthquakes (black circles) recorded at WMQ. Results without (open symbols) and with distance correction (filled symbols) are shown; the latter shows the earthquake and explosion populations to be well separated. Differences in skewness are therefore useful for source discrimination.

7. Conclusions

Our analysis of regional data from nuclear explosions from both NTS and KTS and nearby earthquakes suggests the following conclusions:

(1) There are several reliable source discrimination methods based on the use of only Lg at regional distances. These should be especially useful for small magnitude seismic events for which Lg may be the only well recorded seismic phase.

(2) In this study, our analysis of both NTS and KTS nuclear explosions and nearby earthquakes indicates four possible regional discriminants: (a) normalized standard deviation derived from spectrograms, (b) Lg spectral ratios, (c) Lg spectral slopes, and (4) skewness of Lg spectra.

(3) Remarkable similarity of discrimination results from both NTS and KTS nuclear explosions and nearby earthquakes, with entirely different geological settings, indicates that our results should be applicable to other regions of the world.

8. References

Aki, K. and B. Chouet (1975). Origin of coda waves: source, attenuation, and scattering effects, J. Geophys. Res. 80, 3322-3342.

Aguilar-Chang, J. and M.L. Begnaud (2003). Data Warehouses in Support of Nuclear Explosion Monitoring Research, Proceedings 25th Seismic Research Review, 657-663.

Anderson, D.N. and S.R. Taylor (2002). Application of Regularized Discrimination Analysis to regional seismic event identification, Bull. Seism. Soc. Am. 92, 2391-2399.

Anderson, D.N., S.R. Taylor, K.K. Anderson (1999). Quadratic negative evidence discrimination, Bull. Seism. Soc. Am. 89, 648-656.

Bonner, J. L., H. J. Patton, A. C. Rosca, H. Hooper, J. Orrey, M. Leidig, and I. Gupta (2003). Aspects of Rg and Lg generation from the Shagan Depth of Burial explosions, Proceedings 25th Seismic Research Review, 384-393.

Chael, E. P. (1988). Spectral discrimination of NTS explosions and earthquakes in the southwestern United States using high-frequency regional data, Geophys. Res. Lett. 15, 625-628.

Gitterman, Y., V. Pinsky, A. Shapira, M. Ergin, D. Kalafat, G. Gurbuz, and K. Solomi (2002). Improvement in Detection, Location, and Identification of Small Events through Joint Analysis by Seismic Stations in the Middle East/Eastern Mediterranean Region, Proceedings 24th Seismic Research Review, 271-282.

Gupta, I. N., W. Chan, and R. Wagner (1992). A comparison of regional phases from underground nuclear explosions at East Kazakh and Nevada Test Sites, Bull. Seismol. Soc. Am., 82, 352-382.

Gupta, I.N., C.S. Lynnes, T. W. McElfresh and R. A. Wagner (1990). F-k analysis of NORESS array and single-station data to identify sources of near-receiver and near-source scattering, Bull. Seism. Soc. Am. 80, 2227-2241.

Gupta, I. N. and R. A. Wagner (1998). Study of low and high frequency Lg from explosions and its application to seismic monitoring of the CTBT, AFRL-VS-HA-TR-98-0038, Air Force Research Laboratory, Hanscom Air Force Base, Massachusetts.

Gupta, I. N., T. Zhang, and R. Wagner (1997). Low-frequency Lg from NTS and Kazakh nuclear explosions—Observations and interpretation, Bull. Seismol. Soc. Am., 87, 1115-1125.

Hartse, H. E., W. S. Phillips, M. C. Fehler, and L. S. House (1995). Single-station spectral discrimination using coda waves, Bull. Seism. Soc. Am. 85, 1464-1474.

Hartse, H. E., S. R. Taylor, W. S. Phillips, and G. E. Randall (1997). A preliminary study of regional seismic discrimination in central Asia with emphasis on western China, Bull. Seism. Soc. Am. 87, 551-568.

Jiao, W. and W. Chan (2003). Broadband Seismic Experiments in Southwest and Northeast China, Proceedings 25th Seismic Research Review, 63-72.

Kim, W.-Y., V. Aharonian, A.L. Lerner-Lam, and P.G. Richards (1997). Discrimination of Earthquakes and Explosions in Southern Russia Using Regional High-Frequency Three-Component Data from the IRIS/JSP Caucasus Network, Bull. Seismol. Soc. Am., 87, 569-588.

Myers, S. C., J. Wagoner, S. Larsen, A. Rodgers, K. Myeda, K. Smith, and W. Walter (2003). Simulation of Regional Explosion S-phases (SIRES) project, Proceedings 25th Seismic Research Review, 117-124.

Ortiz, A. M., S. R. Taylor, T. J. Fitzgerald, and T. Wallace (2002). Rediscovering signal complexity discriminants: a preliminary study for application to regional seismic and radio frequency signatures, LA-UR-02-7657, Los Alamos National Laboratory, Los Alamos, NM.

Patton, H. J. (1990). Characterization of spall from observed strong ground motions on Pahute Mesa, Bull. Seism. Soc. Am. 80, 1326-1345.

Patton, H. J. (2000). Ms: mb relationships for small magnitude events: Observations and physical basis for mb based on regional phases, in Proceedings of the 22nd Annual DoD/DOE Seismic Research Symposium, 12-15 September 2000, New Orleans, LA, Volume II, 293- 299.

Patton, H. J. (2001). Regional magnitude scaling, transportability, and Ms: mb discrimination at small magnitudes, Pure appl. geophys., 158, 1951-2015.

Patton, H. J., and S. R. Taylor (1995). Analysis of Lg spectral ratios from NTS explosions: Implications for the source mechanisms of spall and the generation of Lg waves, Bull. Seismol. Soc. Am., 85, 220-236.

Springer, D. L., G. A. Pawloski, J. L. Ricca, R. F. Rohrer, and D. K. Smith (2002). Seismic source summary for all U.S. below-surface nuclear explosions, Bull. Seism. Soc. Am. 92, 1806-1840.

Taylor, S.R. and H.E. Hartse (1997). An evaluation of generalized likelihood ratio outlier detection to identification of seismic events in western China, Bull. Seism. Soc. Am. 87, 824-831.

Taylor, S. R., N. W. Sherman, and M. D. Denny (1988). Spectral discrimnation between NTS explosions and western United States earthquakes at regional distances, Bull. Seism. Soc. Am. 78, 1563-1579.

Walter, W. R., K. M. Mayeda, and H. J. Patton (1995). Phase and spectral ratio discrimination between NTS earthquakes and explosions. Part1: empirical observations, Bull. Seism. Soc. Am. 85, 1050-1067.

Woods, B. B. and D. V. Helmberger (1997). Regional seismic discriminants using wave-train energy ratios, Bull. Seism. Soc. Am. 87, 589-605.

Wu, R. S., X. B. Xie, Z. Ge, X. Wu, and T. Lay (2003). Proceedings 25th Seismic Research Review, 172-181.